INTERACTION OF HIGH-INTENSITY LASER BEAM WITH STRUCTURED SOLID SURFACE PLASMA FOR WAKEFIELD ACCELERATION

B. Lei*, C. Welsch[1], H. Zhang[1], University of Liverpool, Liverpool, United Kingdom
G. Xia[1], University of Manchester, Manchester, United Kingdom
J. Resta-Lopez, Universidad Europea de Valencia, Valencia, Spain
A. Bonatto, Universidade Federal de Ciências da Saúde de Porto Alegre, Porto Alegre, Brazil
[1]also at Cockcroft Institute, Daresbury, United Kingdom

Abstract

Recent research into the interaction between high-intensity beams and surface plasmas has revealed the significant potential for generating extremely strong (TV/m) fields for particle acceleration and radiation production. By overcoming several longstanding challenges in beam–solid interactions, this emerging approach opens new opportunities to extend the energy frontier of particle physics while enabling the development of next-generation micro-scale accelerator facilities with unprecedented flexibility. At the same time, it provides new insights into the highly complex nonlinear dynamics of surface plasmons (SPs) under strong-field conditions and establishes a previously unexplored regime of plasma-based particle acceleration. In this study, we theoretically and numerically investigate high-intensity laser-driven excitation of relativistic surface plasmons (RSPs) on micro-scale smooth surfaces for high-gradient wakefield generation by using particle-in-cell (PIC) simulations. Sub-TeV/m-level leaky and bubble wakefields are shown to be driven by a TW laser with high energy efficiency, enabling the acceleration of both electrons and positrons. These results provide a new pathway toward the development of ultrahigh-gradient, ultra-compact particle accelerators for a broad range of scientific and technological applications.

INTRODUCTION

The current state-of-the-art laser-driven gaseous plasma-based accelerators practically work with a low-density classical plasma in the range of $n_e \sim 10^{14-18}\mathrm{cm}^{-3}$ [1, 2]. This density can, in principle, support an acceleration gradient of approximately $G \sim 1 - 100$ GeV/m. While the recent progress of laser-driven plasma wakefield acceleration (LWFA) mainly benefits from the rapid development of high-power lasers, it is still very challenging to further increase the beam energy. A higher-power laser pulse can introduce very strong nonlinear instabilities during the laser-plasma interaction that degrade the qualities of the plasma wakefield [3]. Although a higher-density plasma n_p can sustain a higher acceleration gradient G_z as $G_z \propto \sqrt{n_p}$, the total energy gain is decreased due to the limited laser penetration, which depends on the laser wavelength λ_0 via the critical density $n_c = m_e c^2/4\pi e^2 \lambda_0^2$ and scales the maximum energy gain as

$$\Delta\mathscr{E}_{\max}[\mathrm{GeV}] \simeq 1.7 \left(\frac{P[\mathrm{TW}]}{100}\right)^{1/3} \left(\frac{10^{18}}{n_p[\mathrm{cm}^{-3}]}\right)^{2/3} \cdot \left(\frac{0.8}{\lambda_0[\mu m]}\right)^{4/3},$$

where P denotes the laser power. m_e and e denote the rest mass and charge of an electron, respectively. c is the speed of light in vacuum. Another major challenge in applying LWFA toward high-energy colliders is the efficient acceleration of positrons, which experience transverse defocusing inside the plasma cavity formed in a uniform plasma [4].

Beyond gaseous plasma-based accelerators, the solid-state plasma accelerator is a promising direction to provide both an extremely high acceleration gradient and a stable field structure for particle acceleration. Recent progress in high-power laser-driven, grating-free RSPs on a metallic surface has opened a new route toward ultra-high gradient, ultra-compact plasma-based particle acceleration and radiation generation [5]. In these schemes, as the laser propagates in the vacuum while interacting with the high-density surface plasma, it then enables stable laser propagation, ultrahigh wakefield, high energy efficiency and flexible structures for field control and beam modulation. Particularly, in this approach, RSPs are excited on the smooth surface instead of the grating surface typically used for conventional SP excitation. Therefore, these methods are intrinsically suitable for high-intensity laser-driven SPs excitation. In the grating-free scheme, RSPs are excited when an intense laser pulse interacts with a finite or curved solid surface, with the coupling efficiency determined primarily by the modal overlap between the incident laser field and the SP eigenmode. As the surface geometry intrinsically governs the SP eigenmodes, this approach enables precise mode selection and controlled manipulation of the excitation dynamics.

The nanostructured low-density vertically-aligned carbon nanotube (VCNT) is proposed to be the platform to support these strong RSP [6–10]. These materials can provide excellent thermal and electronic properties, large-area uniformity, high damage thresholds and well-tailorable geometry as shown in Fig. 1 (b)-(f). More importantly, they can provide a flexible effective surface plasma density down to 10^{19} cm^{-3} that is critical for efficiently supporting the resonance RSP excitation.

* bifeng.lei@liverpool.ac.uk

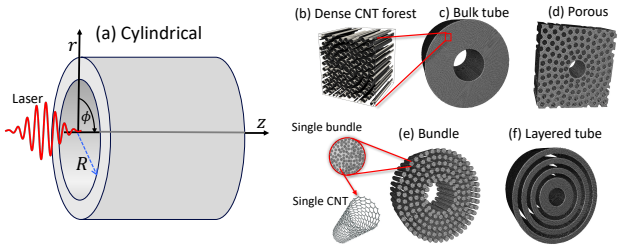

Figure 1: (a) Illustration of cylindrical geometry for RSP excitation. A laser pulse (red) propagates along the axis of a microtube to drive the RSP-based wakefield. The radius of the microtube is R. The cylindrical coordinate is (r, z, ϕ). The vacuum region is inside the cylinder $r < R$ and plasma $r > R$. (b)-(f) Illustration nanostructed VCNT targets design.

SURFACE PLAMON-BASED WAKEFIELD EXCITATION

In classical physics, excitation of RSPs is a process of stimulated Raman scattering (SRS), which can be described by Maxwell's equations and the cold fluid equation with boundary conditions in cylindrical geometry, as shown in Fig. 1 [11]. With the linear surface plasmon response, the wave equation of the electric component E of the RSP field is given as

$$\left[\nabla \times \nabla \times -k_0^2 \varepsilon(\omega)\right] E = i\frac{4\pi\omega}{c^2} J_{\text{ext}}, \tag{1}$$

where $\varepsilon(\omega)$ is the relativistic Drude permittivity in plasma as

$$\varepsilon_2(\omega) = 1 - \frac{\omega_p^2}{\gamma_q \omega^2}. \tag{2}$$

In the eigenmode calculation, γ_q can be treated as a frozen cycle-averaged parameter evaluated at the relevant surface or overlap region. The equation of the eigenfield is then written as

$$\left[\frac{1}{r}\frac{d}{dr}\left(r\frac{d}{dr}\right) - \frac{m^2}{r^2} - \kappa_j^2\right] E_{z,m}^{(j)} = 0, \tag{3}$$

where m represents the azimuthal index of RSP eigenmode. κ_1 and κ_2 are the decay parameters, defined as

$$\kappa_j(\omega, k_z) = \sqrt{k_z^2 - \varepsilon_j(\omega) k_0^2}. \tag{4}$$

Here j is either 1 or 2, denoting the solutions in vacuum or plasma, respectively. k_z is defined as the propagation constant of the surface mode along z and depends on the surface geometry. k_0 denotes the vacuum wavenumber. For the bound surface mode, $\Re\kappa_j > 0$ is required. The solution, a TM mode, is given by

$$\begin{aligned} E_{z,m}^{(1)}(r) &= E_0 I_m(\kappa_1 r) \\ E_{z,m}^{(2)}(r) &= E_0 \frac{I_m(\kappa_1 R)}{K_m(\kappa_2 R)} K_m(\kappa_2 r). \end{aligned} \tag{5}$$

The evanescent nature of the RSP field is presented by the modified Bessel functions I_m and K_m in vacuum and plasma, respectively. The radial electric field $E_{r,m}^{(j)}$ and azimuthal magnetic field $B_{\phi,m}^{(j)}$ are given as $E_{r,m}^{(j)} = (ik/\kappa_j^2) dE_{z,m}^{(j)}/dr$ and $B_{\phi,m}^{(j)} = (i\omega\epsilon_j k/\kappa_j^2) dE_{z,m}^{(j)}/dr$. Notably, the $m = 0$ mode does not decay to zero in the vacuum channel region, but rather provides an on-axis acceleration field. For a ponderomotive drive, only the $m = 0$ cylindrical mode can be excited. These features are significant for RSP-based wakefield acceleration as shown in Fig. 2.

Fully 3D PIC simulations were done by using WarpX [12] to verify the RSP excitation driven by a high-intensity laser where the ponderomotive force is dominant. As the strong curvature makes higher-order radial effects important, and small curvature allows RSP only to see a locally planar interface, a channel radius should be moderate, as $R = 3.0\,\mu\text{m}$. The electron density of the microtube is 4×10^{20} cm^{-3}. We can assume the microtube is made of a VCNT forest and is initially modelled with neutral uniformly distributed carbon atoms with the inisation energies modified with the CNT properties, including weak π-bond and C-C bond (σ-bond) energies. The thermionic emission of electrons is negligible by assuming room temperature. Field ionisation is implemented using the Ammosov-Delone-Krainov (ADK) method. A Gaussian laser pulse of wavelength $\lambda_L = 0.8\,\mu\text{m}$ is linearly polarised in the y direction and propagates along the axis $x = 0\,\mu\text{m}$ in the z direction. It is focused at $z = 0\,\mu\text{m}$ with root-mean-square (RMS) waist $w_0 = 3.0\,\mu\text{m}$ and duration $\sigma_\tau = 6.0$ fs. The dimensions of the moving window are $12\,\mu\text{m} \times 12\,\mu\text{m} \times 20\,\mu\text{m}$, comprising $384 \times 384 \times 512$ cells in the x, y, and z directions, respectively. Each cell contains 8 macro particles, which are sufficient to solve the electron dynamics effectively.

Here, we first identify two regimes, including the leaky and bubble wakefield. The leaky wakefield is excited when the laser strength is not sufficient to drive the electrons to escape from the surface. Only the electromagnetic (EM) field leaks into the vacuum channel and generates a quasi-state field which is capable of accelerating both negatively and positively charged particles, as shown in Fig. 2 (a) and (b). In this regime, self-injection is typically not observed. When the laser strength is sufficiently high to drive the electrons to freely cross the surface, a bubble wakefield is excited. The wakefield is similar to that of a laser-driven bulk plasma bubble, and self-injection is possible, as shown in Fig. 2 (c) and (d). The wakefield has the amplitude of 0.3 TV/m and 0.65 TV/m in the leaky and bubble regimes, respectively. The penetration distance of the laser pulse is only limited by the in-pulse energy and target length. It therefore promises high energy efficiency.

LEAKY WAKEFIELD ACCELERATION AND EDGE-INJECTION

The leaky wakefield has a quasistatic structure which is capable of accelerating both electron and positron beams, as shown in Fig. 2(a) and (b), where the transverse field vanishes from the axis. In PIC simulations, we externally inject either an electron or positron witness beam in the

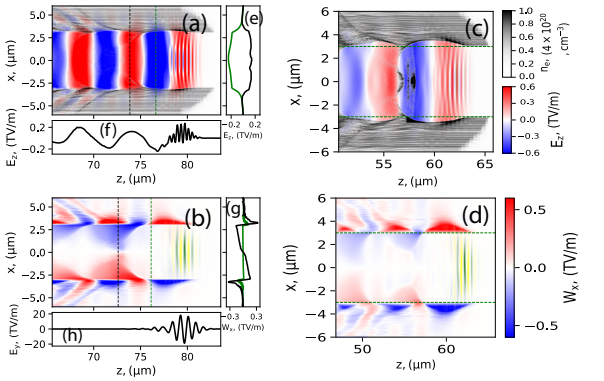

Figure 2: RSP-based wakefield excitation. (a) and (b) longitudinal E_z and transverse $W_x = E_x - cB_y$ component of leaky wakefield where $a_0 = 4.0$. (c) and (d) are corresponding components of bubble wakefield where $a_0 = 10.0$. (e) and (g) are line plots of (a) and (b) along the dashed lines, respectively. (f) and (h) are line plots along the axis in (a) and (b).

proper phase, as indicated by the green or black dashed line in Fig. 2(a) and (b). Both of the beams have the same parameters except for the negative or positive charge, as summarised in Table.1. The evolution of energy gain and beam size is shown in Fig. 3 (a) and (b), where all the electrons and positrons are preserved by the transverse field during the 150 μmlong propagation. The electron gain $\Delta E = 25$ MeV, indicating the mean energy gain rate of $R_E = 0.17$ TeV/m. The positron beam gains $\Delta E = 19$ MeV energy, indicating the mean energy gain rate of $R_E = 0.13$ TeV/m.

Table 1: Parameters of the witness positron and electron beams used in simulations

Beam profile	Gaussian
Charge, Q_{e^+,e^-}	± 1 pC
Beam energy, E	200 MeV
Beam RMS size, σ_r	1.5 μm
Beam RMS duration, σ_τ	1.6 fs
Energy spread	1.0%

The self-injection of electrons is possible in the leaky wakefield during the scattering process of the laser with the vertical edge if the laser strength can be moderately increased [7]. The electrons can be correctly injected into the acceleration phase during the laser scattering with the vertical edge. The duration of the injected electron beam is typically in sub-fs with a very narrow energy spectrum.

SELF-INJECTION AND BUBBLE WAKEFIELD ACCELERATION

In the bubble wakefield region, the self-injection of electrons is similar to that in LWFA, as shown in Fig. 2(c). The longitudinal phase space of the self-injected electron beam and the corresponding energy spectrum are shown in Fig. 3(c) and (d). The energy spectrum extends to 35 MeV after 82 μm propagation, indicating the peak acceleration gradient of $G_{\text{peak}} = 0.43$ TeV/m. The energy spectrum

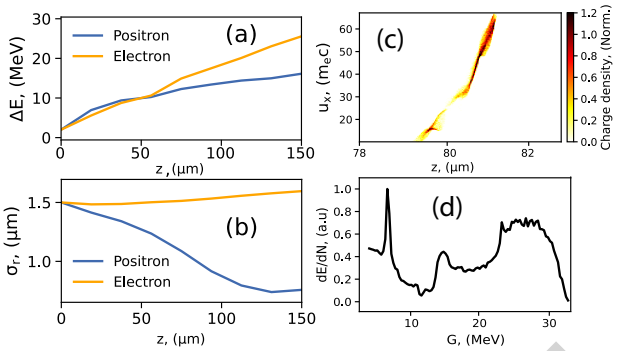

Figure 3: (a) and (b) Evolution of energy gain and beam size of electron and positron beam externally injected in the leaky wakefield where $a_0 = 4.0$. (c)-(d) Longitudinal phase space of the self-injected plasma electrons and the corresponding energy spectrum in the bubble regime where $a_0 = 10.0$. PIC simulations are done with the same parameters as those in Fig. 2 (a) and (b), except a_0.

is broad as electrons continuously transit across the inner surface until the laser pulse is sufficiently depleted, allowing the self-injection process to persist. The high-energy component peaks at 30 MeV with a 26 % spread, while the low-energy component peaks at 5.4 MeV with a 1 % spread. This self-injection mechanism is feasible with currently available high-power laser facilities, offering a possible way for experimental demonstration.

CONCLUSION

In this paper, we demonstrate theoretically and numerically that an RSP-based plasma wakefield can be excited by a high-intensity laser interacting with a smooth cylindrical surface. The dynamical behaviour differs significantly from that observed on a planar surface. The EM field of the surface plasmon can reach amplitudes of sub-TeV/m with a 10 s of TW laser, enabling highly efficient particle acceleration. We identified two plasma-wakefield mechanisms for the acceleration of both negatively and positively charged particles: leaky and bubble wakefields in a microtube. Additionally, we propose the low-density VCNT-based target as the platform to support these high-gradient RSP excitation, benefiting from their excellent properties. However, the complex dynamics of RSP excitation under strong-field conditions remain incompletely understood. Substantial further effort in theory and simulation is still required to effectively guide the successful implementation of proof-of-concept experiments.

REFERENCES

[1] E. Adli *et al.*, "Acceleration of electrons in the plasma wakefield of a proton bunch", *Nature*, vol. 561, no. 7723, pp. 363–367, 2018. doi:10.1038/s41586-018-0485-4

[2] A. J. Gonsalves *et al.*, "Petawatt laser guiding and electron beam acceleration to 8 gev in a laser-heated capillary discharge waveguide", *Phys. Rev. Lett.*, vol. 122, no. 8, p. 084801, Feb. 2019. doi:10.1103/PhysRevLett.122.084801

[3] E. Esarey, C. B. Schroeder, and W. P. Leemans, "Physics of laser-driven plasma-based electron accelerators", *Reviews of Modern Physics*, vol. 81, pp. 1229–1285, 2009. doi:10.1103/RevModPhys.81.1229

[4] G. J. Cao, C. A. Lindstrøm, E. Adli, S. Corde, and S. Gessner, "Positron acceleration in plasma wakefields", *Phys. Rev. Accel. Beams*, vol. 27, no. 3, p. 034801, Mar. 2024. doi:10.1103/PhysRevAccelBeams.27.034801

[5] A. McCay *et al.*, "Surface wave electron acceleration from flat foils at parallel laser incidence", *Phys. Rev. Lett.*, vol. 135, no. 14, p. 145001, Oct. 2025. doi:10.1103/y29y-f63h

[6] A. Bonatto *et al.*, "Exploring ultra-high-intensity wakefields in carbon nanotube arrays: an effective plasma-density approach", *Physics of Plasmas*, vol. 30, no. 3, p. 033105, Aug. 2023. doi:10.1063/5.0134960

[7] B. Lei *et al.*, "Leaky surface plasmon-based wakefield acceleration in nanostructured carbon nanotubes", *Plasma Physics and Controlled Fusion*, vol. 67, no. 6, p. 065036, 2025. doi:10.1088/1361-6587/ade00a

[8] B. Lei *et al.*, "100 s TeV/m-level particle accelerators driven by high-density electron beams in micro structured carbon nanotube forest channel", *New J. Phys.*, vol. 27, no. 8, p. 084301, 2025. doi:10.1088/1367-2630/adf87d

[9] B. Lei *et al.*, "Coherent synchrotron radiation by excitation of surface plasmon polariton on near-critical solid microtube surface", *Phys. Rev. Lett.*, vol. 135, no. 20, p. 205001, Nov. 2025. doi:10.1103/cnym-16hc

[10] C. Bonţoiu *et al.*, "Numerical study of self-injected electron acceleration in cnt structured targets driven by an 800 nm laser", *Sci. Rep.*, vol. 15, no. 1, p. 45323, 2025. doi:10.1038/s41598-025-29386-4

[11] J. Resta-López, A. Bonatto, G. Xia, B. Lei, and C. Welsch, "Surface plasmons in strong fields and their applications to beam acceleration", in *Plasma Science - Current Developments, Applications, and Future Directions*, J. Resta-López and A. Bonatto, Eds. London: IntechOpen2026-03-26, 2026-01-27. doi:10.5772/intechopen.1013683

[12] J.-L. Vay *et al.*, Blast-warpx/warpx: 25.10, Oct. 2025. doi:10.5281/zenodo.17261711